Theoretical understanding of the quasiparticle parity lifetimes reported in WP2

Author	Affiliation	Email
Alfredo Levy Yeyati	UAM	a.l.yeyati@uam.es
Marcelo Goffman	CEA-SACLAY	marcelo.goffman@cea.fr
Project Number	**Project Start Date**	**Duration**
828948	01.04.2019	48 Months
Classification		
	PU	
File Name		
WP No	**Work Package Name**	
5	Supporting theory	
Deliverable No	**Deliverable Name**	
D5.3	Theoretical understanding of the quasiparticle parity lifetimes reported in WP2	
	Approved by	
	Steering Committee of the action	

The opinions expressed in the document are of the authors only and no way reflect the European Commission's opinions. The European Union is not liable for any use that may be made of the information. This project has received funding from the European Union's Horizon 2020 research and innovation programme under grant agreement No 828948.

DOCUMENT REVISION HISTORY

Revision	Date	Description	Author
1.0			

Table of Contents

1. **Introduction**

The Andreev levels parity dynamics have by now been explored experimentally both in atomic contacts [Zgirski2011,Bretheau2013,Janvier2015,Tosi2021] and in semiconducting nanowire junctions [Hays2018]. Deliverable 5.1 was based on unpublished data from the Saclay group on atomic contacts [Tosi2021]. The theoretical analysis presented there considered the case of a short junction hosting one pair of spin degenerate Andreev states and identified the coupling to photons in the resonator and with phonons in the leads as the main source of relaxation and parity jumps. In the meantime, experiments on semiconducting nanowires have progressed and measurements on the parity dynamics have been performed by the Saclay group. There exists also data from a group in Delft (outside the consortium) that has been presented in the CMD29 minicolloquium that we organized last June. The experimental results from the Saclay node are briefly summarized in Sect. II.

From the point of view of theory, the aim is to extend the short junction analysis to the case of finite length ones that could describe the nanowire junctions. There are two main differences between the short and long junction cases, which could affect the dynamics: the number of Andreev states inside the gap that increases roughly linearly with the length [Bagwell1992], and the splitting of Andreev states due to spin-orbit coupling [Tosi2019]. At present, we have focused only in the first of these effects given that the influence of spin-orbit coupling on the parity dynamics is more subtle and there is still not enough resolution to identify it in the experimental data. Our theoretical approach and main results are described in Sect. III.

2. **Summary of experimental results**

Parity dynamics in semiconducting weak links is generally explored by coupling a phase biased InAs nanowire weak link to a microwave resonator in a circuit quantum electrodynamics architecture, as shown in Fig.1.

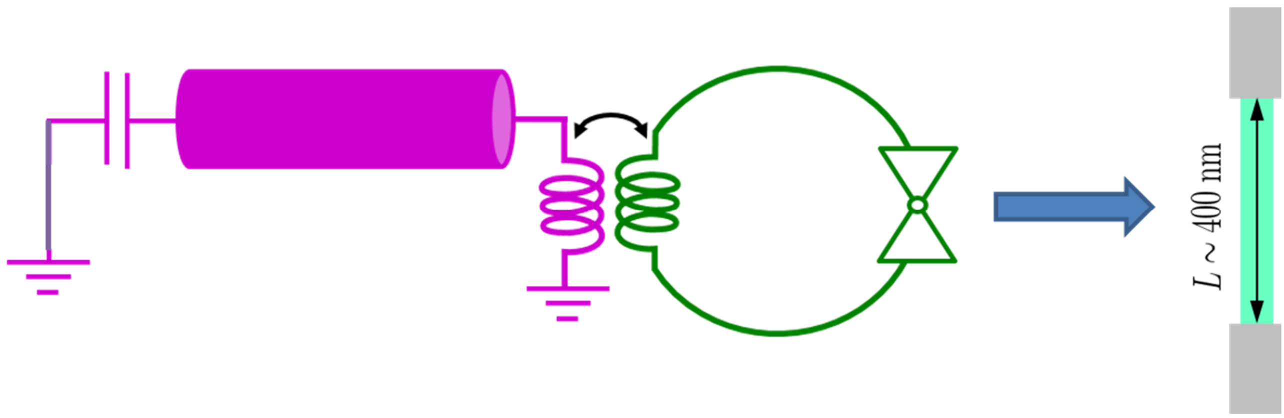

Fig. 1: *Scheme of the setup used to measure the dynamics of Andreev states of a weak link. A phase biased superconducting weak link (green), consisting in a hybrid nanowire junction, is coupled inductively to a microwave resonator (magenta). The resonance frequency of the coupled system encodes information on the population of Andreev states in the weak link. It also provides the main relaxation mechanism considered by our theoretical approach.*

Within this setup, the resonance frequency of the coupled system depends on the occupancy of Andreev levels in the weak link. In particular, changes in the resonance frequency are important for the lowest-lying many-body states of the weak link: the ground "even" state $|g\rangle$, the two single-excited states with odd parity $|o_\sigma\rangle$ ($\sigma = \uparrow, \downarrow$) and the double-excited state with even parity $|e\rangle$. The results reported in this section by the Saclay's node corresponds to data taken at special working points in gate voltage and magnetic flux (known as "sweet spots") with first-order insensitivity to charge and magnetic flux fluctuations. In all sweet spots investigated (at T=11mK), the results show that the steady state of the weak link is a mixed-state of two many-body states: the ground even state, and the odd parity state. The single-shot readout implemented by the Saclay group has not yet allowed to probe the odd-state spin degree of freedom. This is probably because the coupling between the resonator and the phase biased weak link was not strong enough.

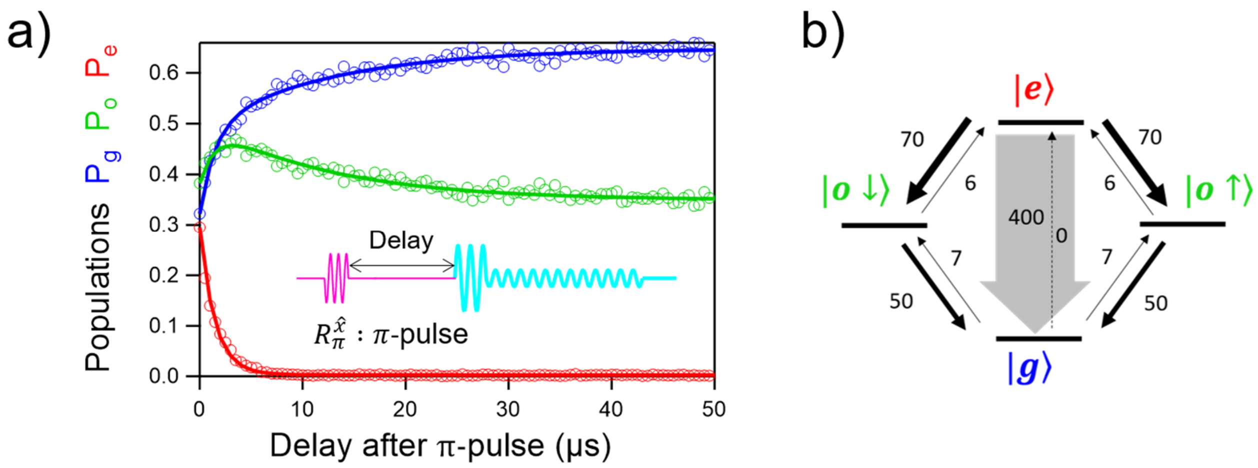

Fig.2 a) The weak link was prepared into $|e\rangle$ state by applying a π-pulse at the transition frequency $f_A = 9.4\ GHz$ (insert). Populations of the states are measured as a function of the delay time after preparation. Solid lines: fit using the rates depicted in Fig2b. b) Rates between states obtained from a master equation. Rates are in ms^{-1}.

Fig.2a shows a relaxation experiment for a nanowire weak link at a typical sweet spot (transition frequency $f_A = 9.4\ GHz$ between $|g\rangle$ and $|e\rangle$). The experimental sequence consist in driving the weak link to prepare it in the $|e\rangle$ state and follow the populations as a function of the delay time after preparation. The results obtained can be adjusted by a master equation with the associated rate between $|g\rangle$, $|o\rangle$ and $|e\rangle$ states (solid lines in Fig.2a). The rates obtained are illustrated in Fig.2b. In this particular case, the observed parity lifetime is around 16μs. Experiments on atomic-size weak links [Janvier2015] reported values close to 30 μs and measurements on similar nanowires [Hays2018, Hays2019] yielded values around 100 μs.

3. Theoretical approach

We base our analysis on the theory developed in Refs. [Olivares2014, Zazunov2014] that we extend to the case of finite length junctions. The situation that we consider is illustrated in Fig.1: a superconducting loop containing the weak link is coupled inductively to a microwave resonator, which acts as a macroscopic electromagnetic environment for the weak link. To determine the dynamics of the Andreev states in the presence phase fluctuations induced by this environment it is necessary to obtain all possible current matrix elements among these states and with the continuum.

For this purpose we model the weak link as a single channel of finite length L between two superconducting leads [Bagwell1992]. The linearized Bogolibov de Gennes equations for this model in the basis $\boldsymbol{\Psi}(\boldsymbol{x}) = \{\boldsymbol{\Psi}_{eR}(\boldsymbol{x})\ \boldsymbol{\Psi}_{eL}(\boldsymbol{x})\ \boldsymbol{\Psi}_{hR}(\boldsymbol{x})\boldsymbol{\Psi}_{hL}(\boldsymbol{x})\}$, where R(L) refers to the right(left) moving quasi-electrons (e) and quasi-holes (h); reads

$$\begin{pmatrix} H_0 + H_b & \Delta(x) \\ \Delta(x) & -H_0 - H_b \end{pmatrix} \Psi(x) = E\Psi(x)$$

The H_0 term corresponds the kinetic energy, i.e. $H_0 = diag(-i\partial_x - v_F; i\partial_x - v_F)$, $\Delta(x)$ to the pairing potential in the leads, $\Delta(x) = \Delta(\theta(-x) + \theta(x - L))$, and H_b to a delta like potential barrier,

$$H_b = U_0 \delta(x - x_0) \begin{pmatrix} 1 & 1 \\ 1 & 1 \end{pmatrix}$$

The effect of the potential barrier can be included as an additional boundary condition at $= x_0$, $\Psi(x_0 + 0^+) = M_{b,tot} \Psi(x_0 - 0^+)$, with $M_{b,tot} = \ diag\left(e^{-\frac{i\delta}{2}} M_b,\ e^{\frac{i\delta}{2}} M_b\right)$, where δ is the superconducting phase difference and

$$M_b = \frac{1}{t'} \begin{pmatrix} tt' - rr' & r' \\ -r & 1 \end{pmatrix}$$

where t, t' and r, r' are the corresponding transmission and reflection amplitudes for the potential barrier.

By imposing the matching conditions at each interface, we obtain the wave function coefficients on the different regions. In particular, for the bound states we obtain the transcendental equation

$$2 \cos^{-1} \varepsilon \ + 2\lambda\varepsilon \pm \alpha = 2n\pi$$

where $\cos \alpha = \tau cos\delta + R \cos 2\lambda\varepsilon x_r$, $\varepsilon = E/\Delta$, $\lambda = L/\xi$, and $\tau = 1 - R$ is the barrier transmission coefficient. Solving this equation we obtain the dispersion relation for the states shown in Fig. 3.

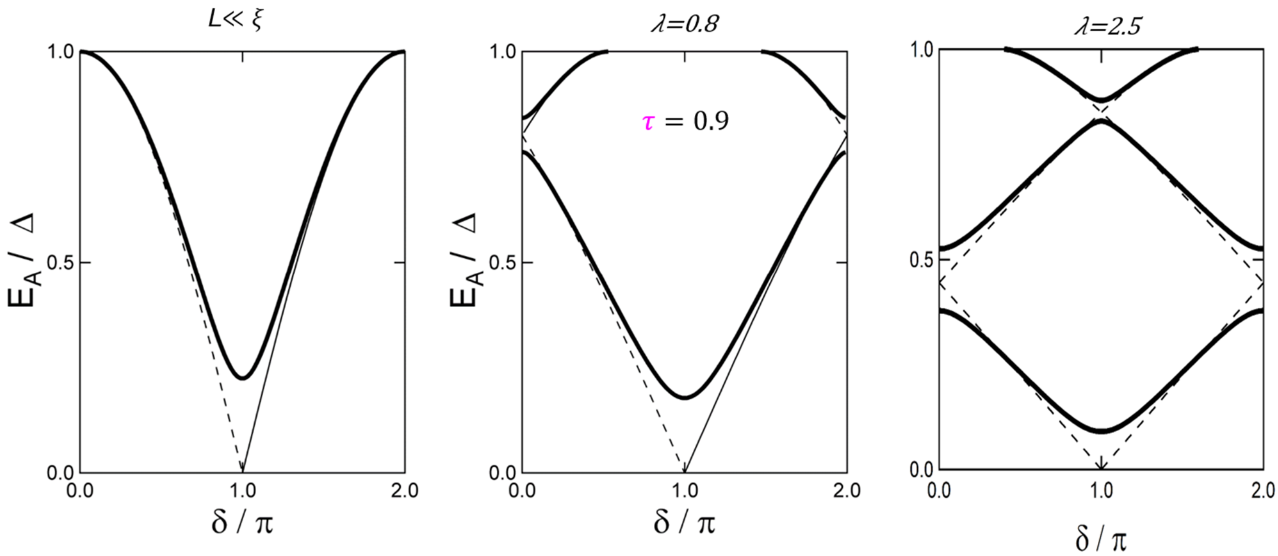

Fig 3: *Andreev bound states spectrum for a weak link of increasing length. The barrier transmission is set at τ=0.9.*

On the other hand, from the wave functions we can obtain the matrix elements for the current operator, which in the present representation adopts a simple form, $I = \frac{\delta(x-x_0)}{2} diag(v_F, -v_F, v_F, -v_F)$. Some results illustrating the behavior of these matrix elements coupling bound and continuum states are shown in Fig. 4.

As can be observed, while the behavior as a function of phase of the current matrix elements is similar for the different lengths, they exhibit a continuous decrease around phase π with length. This is more clearly seen in Fig. 5, where we plot the current matrix elements as a function of length at phase π. Remarkably, the matrix elements $|I_{\varepsilon_1,E}|$ and $|I_{-\varepsilon_1,E}|$ exhibit an inversion around λ~1.3.

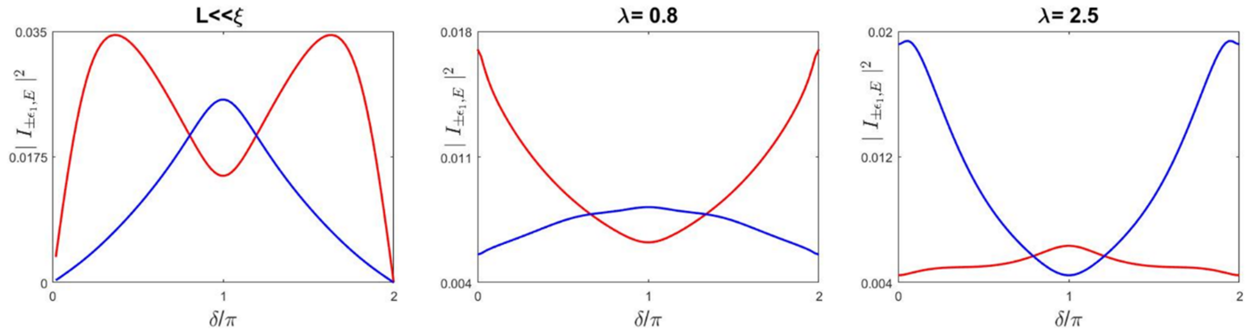

Fig. 4: *Current matrix elements coupling the lower energy Andreev states with continuum ($E = 1.2\Delta$) for the same parameters as in Fig. 3. Red and blue correspond to Andreev state with positive and negative energy respectively.*

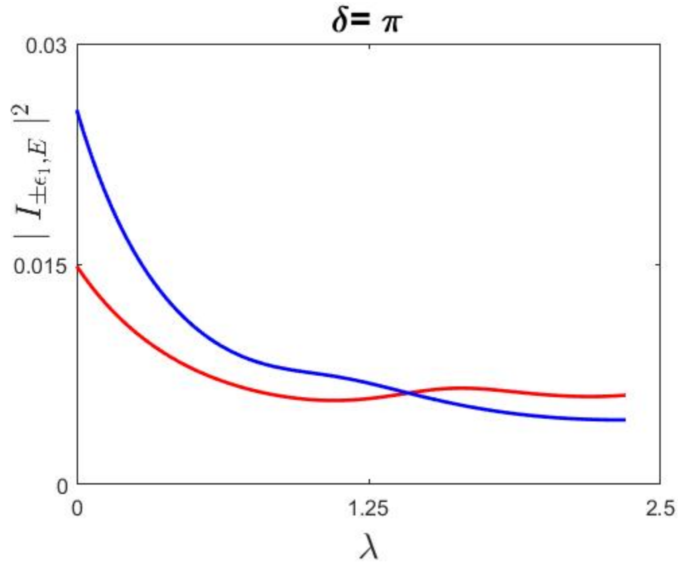

Fig. 5: *Current matrix elements as a function of reduced length λ at phase $\delta = \pi$ (rest of parameters as in Fig. 4).*

Setting up the rate equations

In order to build a rate equation description for the dynamics of the Andreev states subsystem, we follow references [Olivares2014,Zazunov2014] but extended to a situation where more than one Andreev excitation is present, as illustrated in Fig. 6. We should distinguish parity conserving from parity switching transitions, the last ones must necessarily involve quasiparticles in the continuum.

In the case of parity conserving transitions the corresponding rates are given by

$$\Gamma_{\varepsilon_n,\varepsilon_m} = \frac{2\pi}{h}\left|I_{\varepsilon_n,\varepsilon_m}\right|^2 (1 + n_B(\varepsilon_n - \varepsilon_m))J(\varepsilon_n - \varepsilon_m) \ ,$$

where n_B denotes the Bose distribution function for photons in the resonator that we assume to be in thermal equilibrium at a temperature T_{env} and $J(\omega)$ is the environment spectral density, which we approximate as

$$J(\omega) = \frac{\kappa^2\eta_d}{\pi}\left(\frac{1}{(\omega - \Omega)^2 + \eta_d^2} - \frac{1}{(\omega + \Omega)^2 + \eta_d^2}\right)$$

where Ω is the resonator frequency, η_d is the damping for the photons in the resonator and κ determines the coupling to the weak link. On the other hand, for the parity switching transitions, a typical rate like the creation of a continuum quasiparticle at an energy E by the excitation of a trapped quasiparticle in the Andreev states by absorption of a photon would be given by

$$\Gamma_{p,\varepsilon_n} = \frac{2\pi}{h}\left|I_{p,\varepsilon_n}\right|^2 n_B(E-\varepsilon_n)J(E-\varepsilon_n)(1-n_p)\ ,$$

where n_p is the distribution for quasiparticles in the continuum states denoted by p. As a first approach we shall assume that continuum quasiparticles are in thermal equilibrium at a temperature T_{qp}, which can be different from the environmental temperature T_{env}. In a subsequent analysis we could relax this condition and determine the continuum quasiparticles distribution self-consistently as done in [Zazunov2014].

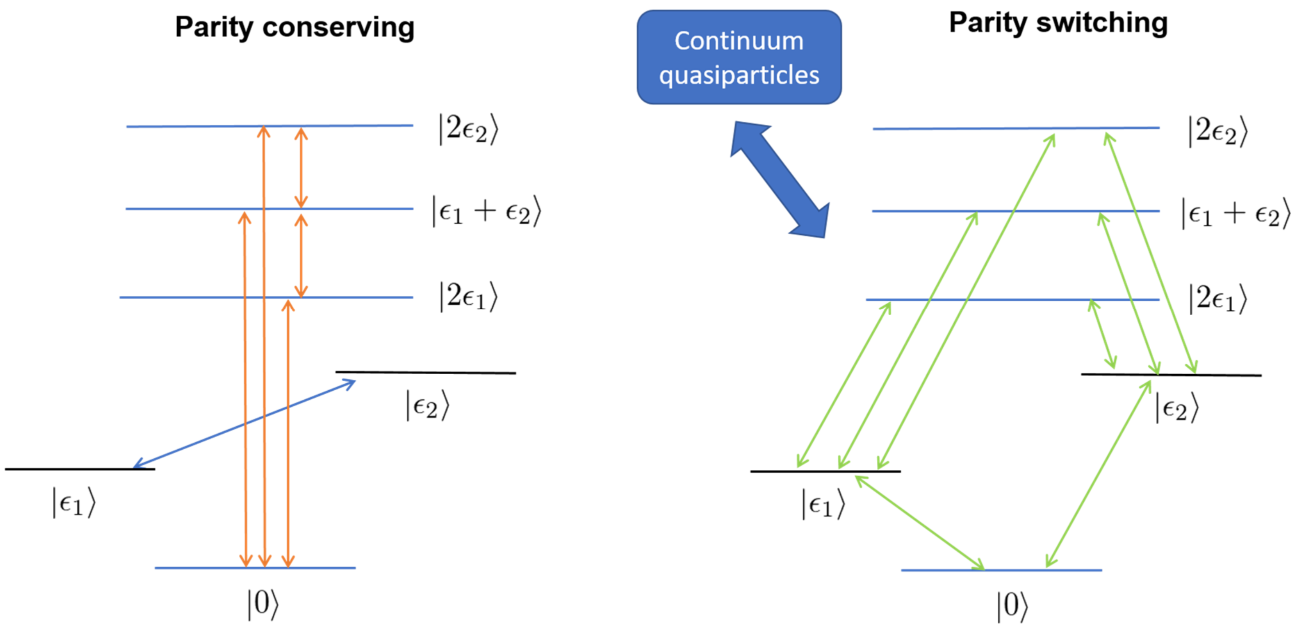

Fig. 6: *Scheme of the parity conserving (left) and parity switching (right) transitions that we consider to analyze the Andreev states dynamics. We focus on the case of an intermediate length weak link with two Andreev states (energies ε_1 and ε_2) inside the gap and neglect the spin degree of freedom.*

Under these conditions and focusing on a case like the one schematized in Fig. 5, with two Andreev states within the gap, we obtain the following rate equations for the populations $\rho_0, \rho_{\varepsilon_1}, \rho_{\varepsilon_2}, \rho_{2\varepsilon_1}, \rho_{\varepsilon_1+\varepsilon_2}$, and $\rho_{2\varepsilon_2}$

$$\begin{aligned}
\dot{\rho_0} &= -\sum_{m,n=1,2} \Gamma_{\epsilon_m,-\epsilon_n}\rho_0 - \Gamma_{-\epsilon_m,\epsilon_n}\rho_{\epsilon_m+\epsilon_n} \\
&\quad -\sum_{p;m=1,2}\left[n_p(\Gamma_{\epsilon_m,p}\rho_0 - \Gamma_{-\epsilon_m,p}\rho_{\epsilon_m}) + (1-n_p)(\Gamma_{p,-\epsilon_m}\rho_0 - \Gamma_{p,\epsilon_m}\rho_{\epsilon_m})\right] \\
\dot{\rho}_{\epsilon_m} &= \Gamma_{\epsilon_m,\epsilon_{\bar{m}}}\rho_{\epsilon_{\bar{m}}} - \Gamma_{\epsilon_{\bar{m}},\epsilon_m}\rho_{\epsilon_m} \\
&\quad + \sum_{p;n=1,2} n_p(\Gamma_{-\epsilon_n,p}\rho_{\epsilon_m+\epsilon_n} - \Gamma_{\epsilon_n,p}\rho_{\epsilon_m} + \Gamma_{\epsilon_m,p}\rho_0 - \Gamma_{-\epsilon_m,p}\rho_{\epsilon_m}) \\
&\quad + \sum_{p;n=1,2}(1-n_p)(\Gamma_{p,-\epsilon_m}\rho_0 - \Gamma_{p,\epsilon_m}\rho_{\epsilon_m} + \Gamma_{p,\epsilon_n}\rho_{\epsilon_m+\epsilon_n} - \Gamma_{p,-\epsilon_n}\rho_{\epsilon_m})
\end{aligned}$$

$$\dot{\rho}_{2\epsilon_m} = \Gamma_{\epsilon_m,-\epsilon_m}\rho_0 - \Gamma_{-\epsilon_m,\epsilon_m}\rho_{2\epsilon_m} - \Gamma_{\epsilon_{\bar{m}},\epsilon_m}\rho_{2\epsilon_m} + \Gamma_{\epsilon_m,\epsilon_{\bar{m}}}\rho_{\epsilon_1+\epsilon_2}$$
$$+ \sum_p [(1-n_p)(\Gamma_{p,-\epsilon_m}\rho_{\epsilon_m} - \Gamma_{p,\epsilon_m}\rho_{2\epsilon_m}) + n_p(\Gamma_{\epsilon_m,p}\rho_{\epsilon_m} - \Gamma_{-\epsilon_m,p}\rho_{2\epsilon_m})]$$

$$\dot{\rho}_{\epsilon_1+\epsilon_2} = \sum_{m=1,2} \Gamma_{\epsilon_m,-\epsilon_{\bar{m}}}\rho_0 - \Gamma_{-\epsilon_{\bar{m}},\epsilon_m}\rho_{\epsilon_1+\epsilon_2} + \Gamma_{\epsilon_{\bar{m}},\epsilon_m}\rho_{2\epsilon_m} - \Gamma_{\epsilon_m,\epsilon_{\bar{m}}}\rho_{\epsilon_1+\epsilon_2}$$
$$+ \sum_{p,m} [n_p(\Gamma_{\epsilon_{\bar{m}},p}\rho_{\epsilon_m} - \Gamma_{-\epsilon_{\bar{m}},p}\rho_{\epsilon_1+\epsilon_2}) + (1-n_p)(\Gamma_{p,-\epsilon_{\bar{m}}}\rho_{\epsilon_m} - \Gamma_{p,\epsilon_{\bar{m}}}\rho_{\epsilon_1+\epsilon_2})]$$

Results on steady state populations

We have solved numerically these equations for the steady state populations. In Fig. 7 we show the evolution of the even and odd states populations as a function of phase difference for the three values of the reduced length $\lambda = 0, 0.8$ and 2.5 in Figs. 2 and 3, and with transmission $\tau = 0.9$. For the resonator parameters we assumed $\Omega = 0.25\,\Delta$ and $\eta_d = 0.01\,\Delta$, as suggested by the experimental situation of Refs. [Tosi2019,Metzger2021], while as a first guess we take $T_{qp} = 0.1\Delta$ and $T_{env} = 0.3\Delta$ as for these temperature values the typical rates are of the order of the ones observed experimentally. As can be observed, in all cases the odd states population becomes significant around $\delta = \pi$, as expected from the ABS dispersion. More remarkably, there is a continued increase of the odd states population with λ which leads to a population inversion between even an odd states for $\lambda = 2.5$.

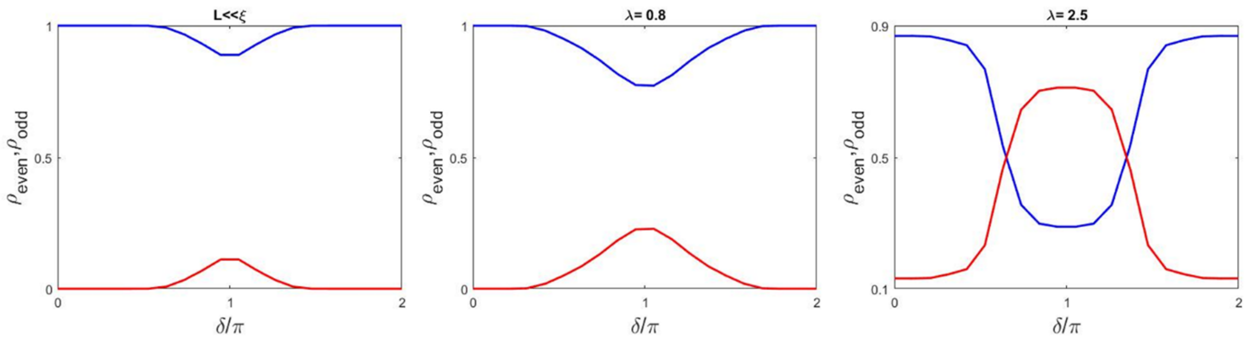

Fig. 7: *Even and odd states population as a function of phase for the three values of λ and the same transmission probability as in Figs. 2 and 3. Rest of parameters as indicated in the text.*

To understand this inversion more clearly, we show in Fig. 8 the evolution of the different states populations as a function of T_{env} and T_{qp} for $\delta = \pi$. We observe that when fixing T_{qp} at 0.1Δ a population inversion between the ground and the $|\varepsilon_1>$ states occurs for $T_{env}\sim 0.1\Delta$ (Fig.8 left panel); whereas the population inversion can be reverted by increasing by increasing T_{qp} above 0.1Δ with T_{env} fixed at 0.1Δ (Fig. 8 right panel).

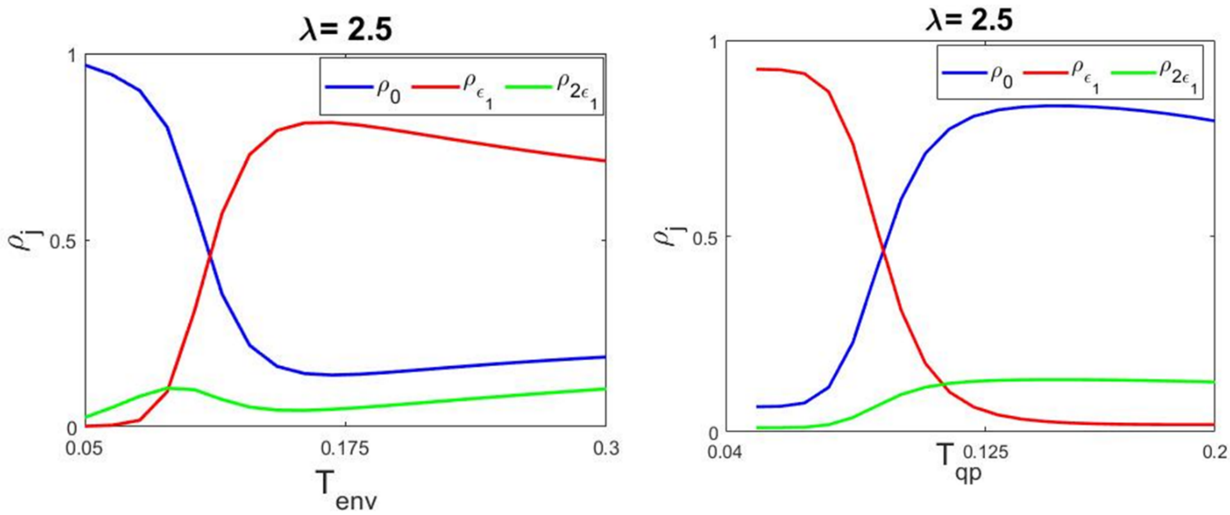

Fig. 8: *Different states populations for* $\lambda = 2.5$, $\tau = 0.9$ *and* $\delta = \pi$ *as a function of* T_{env} *with* T_{qp} *fixed at* 0.1Δ *(left) and as a function of* T_{qp} *with* T_{env} *fixed at* 0.1Δ *(right).*

4. Conclusions

In conclusion, we have extended the theoretical approach of Refs. [Olivares2014,Zazunov2014] for analyzing the parity dynamics to the case of finite length junctions hosting more than one pair of Andreev states. We have considered the coupling to the resonator as the main source for quasiparticle relaxation and found that a population inversion can occur for long enough junctions with high transmissions depending on the parameters T_{env} and T_{qp} controlling the resonator and continuum quasiparticles temperature respectively. On the other hand experiments on the parity dynamics on nanowire junctions conducted by the Saclay node indicate parity lifetimes of the order of 20 μs, somewhat shorter than the values of the order of 100 μs reported by the Yale group in [Hays2018]. While our theory is able to account qualitatively for the observed behavior we have not yet attempted a direct comparison, which would require a more detailed experimental study and probably the inclusion of other relaxation mechanisms within the theory.

References

[Bagwell1992] Philip F. Bagwell, “Suppression of the Josephson current through a narrow, mesoscopic, semiconductor channel by a single impurity”, Phys. Rev. B **46**, 12573 (1992).

[Bretheau2013] L. Bretheau, Ç. Ö. Girit, C. Urbina, D. Esteve, and H. Pothier, “Supercurrent Spectroscopy of Andreev States”, Phys. Rev. X. **3**, 041034 (2013).

[Hays2018] M. Hays, *et al.*, “Direct Microwave Measurement of Andreev-Bound-State Dynamics in a Semiconductor-Nanowire Josephson Junction”, Phys Rev. Lett. **121**, 047001 (2018).

[Hays2020] M. Hays, *et al.*, “Continuous monitoring of a trapped superconducting spin”, Nature Phys. **16**, pages1103–1107 (2020)

[Janvier2015] C. Janvier *et al.,* “Coherent manipulation of Andreev states in superconducting atomic contacts”, Science **349**, 1199-1202 (2015).

[Metzger2021] C. Metzger, Sunghun Park, L. Tosi, C. Janvier, A. A. Reynoso, M. F. Goffman, C. Urbina, A. Levy Yeyati, and H. Pothier, “Circuit-QED with phase-biased Josephson weak links”, Phys. Rev. Research **3**, 013036 (2021).

[Olivares2014] D. Olivares, A. Levy Yeyati, L. Bretheau, C. Girit, H. Pothier and C. Urbina, “Dynamics of quasiparticle trapping in Andreev levels”, Phys. Rev. B. **89**, 104504 (2014).

[Tosi2019] L. Tosi, C. Metzger, M. F. Goffman, C. Urbina, H. Pothier, Sunghun Park, A. Levy Yeyati, J. Nygård, and P. Krogstrup, “Spin-Orbit Splitting of Andreev States Revealed by Microwave Spectroscopy”, Phys. Rev. X **9**, 011010 (2019)

[Tosi2021] L. Tosi *et al.,* in preparation.

[Zazunov2014] A. Zazunov, A. Brunetti, A. Levy Yeyati and R. Egger, “Quasiparticle trapping, Andreev level population dynamics, and charge imbalance in superconducting weak links”, Phys. Rev. B. **90**, 104508 (2014)
[Zgirski2011] M. Zgirski, L. Bretheau, Q. Le Masne, H. Pothier, D. Esteve, and C. Urbina, “Evidence for Long-Lived Quasiparticles Trapped in Superconducting Point Contacts”, Phys. Rev. Lett. **106**, 257003 (2011).